

Influence of Compressed Carbon Dioxide on the Capillarity of the Gas–Crude Oil–Reservoir Water System

Philip T. Jaeger*

Eurotechnica GmbH, An den Stücken 55, D-22941 Bargteheide, Germany

Mohammed B. Alotaibi and Hisham A. Nasr-El-Din

Texas A&M University, Dwight Look College of Engineering, College Station, Texas 77843-3116, United States

The application of carbon dioxide is becoming increasingly important for enhanced oil recovery (EOR) processes. In view of combined EOR and carbon dioxide capture and storage technologies (CCS), knowledge must be gained on relevant properties of the participating fluid mixtures. The solubility of carbon dioxide is significant in many hydrocarbon materials, which affects the capillarity and migration of fluids in oil reservoirs via the interfacial tension (IFT) and wetting of the rock surfaces. For EOR the capillarity is decisive in view of the pressure that has to be overcome within the rock pores. The present study is dedicated to a thorough experimental description of a gas–crude oil–reservoir water system and its behavior under CO₂ pressure including oil density and interfacial properties. The experimental results of decreasing IFT in a three-phase system, increasing density and diminishing wettability, show an important influence of the presence of carbon dioxide.

Introduction

Extensive work has been performed on determining the interfacial tension (IFT) of liquid–gas and liquid–liquid systems containing hydrocarbons and aqueous solutions at reservoir conditions.^{1,2} However, only a few investigations were dedicated toward liquid–liquid–vapor systems,³ including a third phase of considerable lower density. Wetting behavior has been determined under pressure mostly either in pure component liquid–liquid⁴ or liquid–gas systems.⁵ Crude oils are complex mixtures, and in the presence of partly miscible gases, their properties are mostly unknown under reservoir conditions. It is therefore useful to start by investigating fluid mixtures of known phase behavior such as alkanes in atmospheres of CO₂ or methane. The aim of the present study is to extend the database of real reservoir systems for future exploration techniques. Among various properties of fluid mixtures is the IFT, which is important in enhanced oil recovery (EOR). IFT is strongly affected by changing reservoir conditions. In the presence of CO₂, IFT generally decreases to a considerable extent.⁶ At the critical point of the fluid mixture ($P \sim P_c$), IFT approaches zero.⁷ In case of liquids of higher molecular weights, complete miscibility is not achieved at conditions of technical interest. At such elevated pressures IFT may still remain detectable, albeit with low absolute values. Hydrocarbon systems in oil and gas production may show either of the described properties when being contacted with compressed CO₂.

Regarding capillarity in reservoir rock systems the wetting of the participating fluids on the rock surface needs to be taken into account. Several attempts have been carried out to describe the wetting behavior in systems coming as close as possible to the actual reservoir conditions. Sophisticated methods have been proposed to account for aging phenomena of rock surfaces.⁸

Experiments have even been performed at elevated pressures. Nevertheless, the effect of elevated gas pressure has not been entirely understood, especially in liquid–liquid systems. Gas saturation has multiple effects on the three-phase contact angle (CA) by taking influence on the participating interfacial energies.⁹

In the present work, experimental methods are presented to obtain information on these relevant system properties. Findings in this paper will add more knowledge to understanding such interfacial phenomena in complex reservoir systems. The introduced procedure further represents a robust experimental method, which can be adopted by research and development departments to gain a thorough insight into specific complex systems and conditions that are of interest and often far from being accessible by theory and experiments on ideal systems only.

Materials

Sour crude oil was obtained from western Texas. The densities at (313 and 353) K are 0.8288 g·cm⁻³ and 0.7993 g·cm⁻³, respectively. The oil has approximately 0.5 weight fraction of alkanes (*n*-heptane to heneicosane, C21, see Table 1). The remaining part consists mainly of cycloalkanes and aromatics. *n*-Heptane was provided by Sigma Aldrich at a mass fraction of ≥ 0.99 . Volume fractions of the used carbon dioxide, nitrogen, and methane amounted to at least 0.99995.

Calcium carbonate crystals (surface roughness 1.2 μm), limestone (surface roughness 7.7 μm), sandstone (surface roughness 20.2 μm), and dolomite (surface roughness 19.7 μm) outcrop rocks were aged prior to the experiments for up to two months at room temperature using a solution of 1.5 wt % cyclohexanepentanoic acid in *n*-decane, which was also used by Wu et al.¹⁰ Synthetic seawater was prepared according to Table 2.

* Corresponding author. E-mail: jaeger@eurotechnica.de. Fax: +49 4532-267709.

Table 1. Composition of the Crude Oil Used in the Experiments

compound	w
cyclopentane, methyl-	0.0495
cyclohexene	0.0162
heptane	0.0258
cyclohexane, methyl-	0.0709
toluene	0.0838
octane	0.0415
cyclohexane, ethyl-	0.0330
ethylbenzene	0.0749
<i>p</i> -xylene	0.0743
<i>o</i> -xylene	0.0215
nonane	0.0337
benzene, 1-ethyl-3-methyl-	0.0209
decane	0.0585
undecane	0.0389
dodecane	0.0384
tridecane	0.0407
dodecane, 2,6,10-trimethyl	0.0208
tetradecane	0.0306
pentadecane	0.0350
hexadecane	0.0424
heptadecane	0.0268
pentadecane, 2,6,10,14-tet	0.0164
octadecane	0.0240
hexadecane, 2,6,10,14-tet	0.0218
nonadecane	0.0213
eicosane	0.0216
heneicosane	0.0167

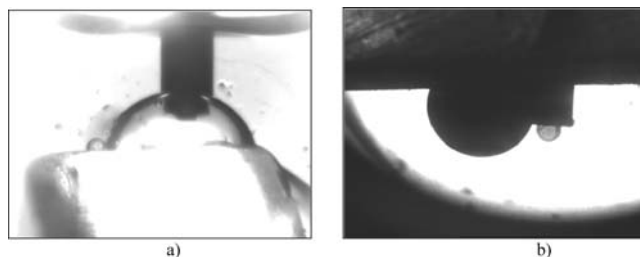
Table 2. Synthetic Seawater (Arabian Gulf, Density at 323.2 K = 1026.8 kg·m⁻³)

ion	concentration/ppm
Na ⁺	10 556
Ca ²⁺	400
Mg ²⁺	1262
Cl ⁻	18 980
HCO ⁻	140
SO ₄ ⁻	2650

Methods

The measurements of IFT and wetting were conducted in high pressure view chambers (Eurotechnica GmbH, Germany, $P_{\max} = 70$ MPa, $T_{\max} = 180$ °C, window diameter 18 mm, SS and Hastelloy C276) allowing for visualization of pendant drops and drops attached to solid surfaces of rock samples that can easily be introduced into the chambers. The principle setup is shown in Figure 1. The measurement procedure is also described by Nasr-El-Din et al.¹¹ Pressure is determined by a pressure transducer (WIKA, Germany) to ± 0.1 MPa. The temperature is measured by a thermocouple type K directly inside the view chamber with an accuracy of 0.1 K.

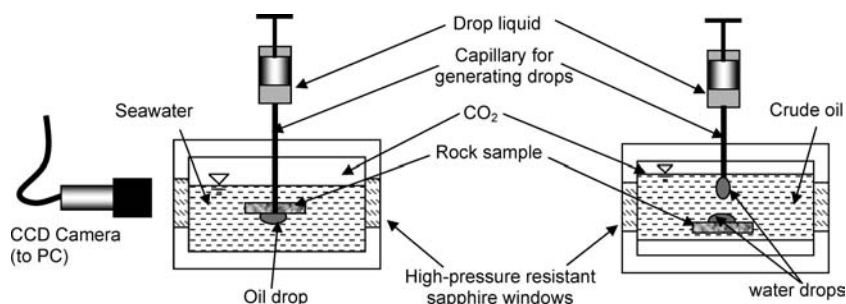
The equipment shown in Figure 1 was used for generating drops of the heavier phase, for example, hydrocarbon liquid in CO₂ or water in oil as well as drops of the lighter phase, that is, hydrocarbon liquids in aqueous solutions. At the beginning of the respective experiment (2 to 3) mL of the drop liquid are

**Figure 2.** Seawater drop on calcium carbonate in crude oil + CO₂ (a), crude oil drop under calcium carbonate in seawater + CO₂ (b), 5.51 MPa, 323.2 K.

pushed through the capillary and collected at the bottom of the chamber to presaturate the surrounding fluid phase. To generate drops of viscous crude oil, a mini-metering unit was installed at the top of the view chamber. The IFT was determined by evaluating the profiles of pendant drops according to the Laplace equation of curved fluid interfaces.¹² In general, the mean value retrieved from at least three different drops is reported. In case of the hydrocarbon–CO₂ system the measurement uncertainty amounts to ± 0.3 mN·m⁻¹. In case water is present, uncertainties increase to ± 0.5 mN·m⁻¹. The density data were retrieved from Kunz et al.¹³ in case of heptane mixtures. In the case of crude oil, densities were determined experimentally (see below). The used densities are reported in the respective tables together with the IFT.

To determine the CA, pieces of rock were cut from core samples and introduced into the view chamber without further treatment of the surface. Calcite crystals rather crack arbitrarily when being cut but nevertheless leave smooth and plane surfaces. According to the conventional method, a sessile drop of water is placed on the surface in the oil phase,¹⁴ determining the CA through the oil phase. Because of the low visibility of the crude oil, the procedure was inverted, especially in those cases where the porous surfaces are water wet, since the drop disappears before obtaining an equilibrium value of the CA. Under these conditions a drop of the lighter crude oil was placed underneath the rock sample as a so-called captive drop. After reaching a constant equilibrium shape the CA was determined through the water phase, which is illustrated in Figure 1, left, and Figure 2, right. The drop volume was in the range of $(20 \text{ to } 25) \cdot 10^{-9}$ m³.

The density is determined from the balance of gravitational and buoyancy forces acting on a liquid element at elevated pressure according to the Archimedes principle. The liquid under consideration is filled into a glass containment (height = 15 mm, ID = 6.5 mm), which is attached to a hook connected to a permanent magnet inside an autoclave of a total volume of 66 mL. The autoclave is pressurized with the gas under consideration. To minimize extraction from the liquid sample into the surrounding CO₂ phase, the entering CO₂ is saturated

**Figure 1.** Setup for determining the CA of liquid–liquid–vapor systems using the sessile drop technique at elevated pressures.

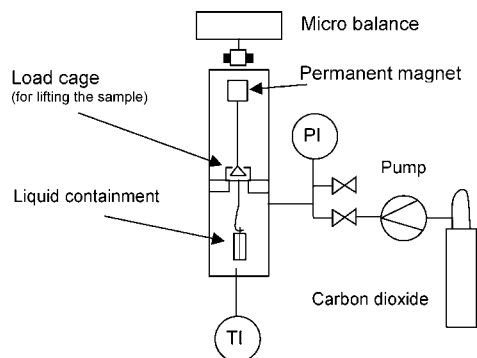


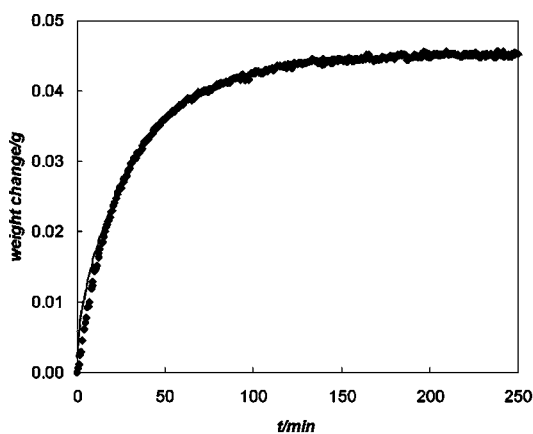
Figure 3. Setup for determining weight changes of liquids in a compressed gas atmosphere.

by passing the surface of about 5 mL of the same liquid in the bottom of the autoclave. The weight of the glass containment including the sample liquid results from its mass and the buoyancy originating from the surrounding fluid mixture. This weight is detected via a magnetic coupling by a microbalance on the outside of the autoclave and recorded by a personal computer, which also controls the magnetic coupling. This so-called magnetic suspension balance (Rubotherm, Germany, $P_{\max} = 35$ MPa, $T_{\max} = 120$ °C) is placed inside a heating air bath for temperature equilibration within ± 0.5 K. The change in the volume of the oil was detected by visual observation through high-pressure sapphire windows. The principle setup is depicted in Figure 3.

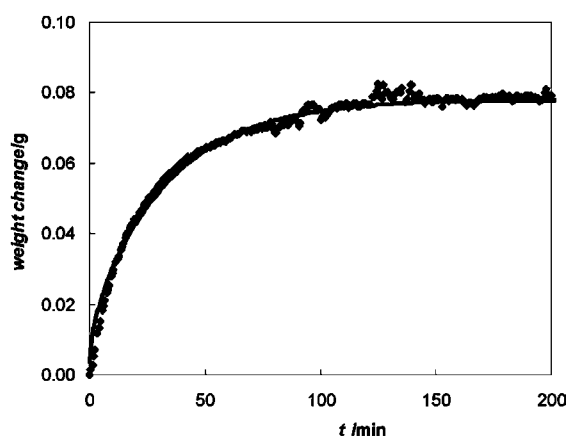
Results

The experimental results are divided into density of crude oil saturated with CO_2 , IFT and wetting behavior. The section on IFT covers observations on single fluids and complex multiphase systems. In the case of the wetting experiments, up to four phases were noted.

Density of Crude Oil Saturated with CO_2 . The density of crude oil was investigated using the gravimetric method described previously by exposing the oil to carbon dioxide at different pressures. Figure 4 shows the kinetics of gas sorption into the crude oil. At the beginning, dissolution is fast, leveling out after nearly two hours when the crude oil becomes increasingly saturated. Taking into account changing buoyancy by increasing volume of the oil phase, the change in density due to saturation with CO_2 is determined as the difference



(a)



(b)

Figure 4. Change of mass due to the dissolution of carbon dioxide in crude oil at 313.2 K. (a) $P = 4.0$ MPa; (b) $P = 6.1$ MPa.

Table 3. IFT of *n*-Heptane in Different Gas Atmospheres^a

vapor phase	T K	P MPa	ρ_{liquid} $\text{kg} \cdot \text{m}^{-3}$	ρ_{gas} $\text{kg} \cdot \text{m}^{-3}$	IFT $\text{mN} \cdot \text{m}^{-1}$		
N_2	323.2	0.1	658.3	1.04	17.6 ± 0.2		
		3.4	662.1	35.4	16.0 ± 0.2		
		6.9	666.0	71.4	13.7 ± 0.2		
		10.4	669.6	106.5	12.0 ± 0.1		
		0.1	679.1	0.86	19.8 ± 0.2		
CH_4	298.2	1.0	673.7	6.86	18.0 ± 0.2		
		2.0	667.3	13.8	16.5 ± 0.2		
		3.0	660.5	20.9	15.0 ± 0.2		
		4.0	653.3	28.4	13.4 ± 0.2		
		6.0	638.0	44.2	10.1 ± 0.2		
		8.0	621.6	61.2	7.9 ± 0.2		
		1	604.2	79.5	5.8 ± 0.1		
		15.0	555.6	131.5	2.3 ± 0.1		
		CO_2	323	0.1	657.0	1.6	16.8 ± 0.2
				3.1	661.0	59.4	10.1 ± 0.2
4.5	683.8			93.7	7.8 ± 0.2		
5.5	707.9			123.2	5.7 ± 0.1		
7.9	738.0			231.7	1.5 ± 0.08		
9.3	578.2			421.3	0.11 ± 0.03		
353	0.1			631.0	1.5	13.6 ± 0.2	
	2.1			621.3	35.4	10.6 ± 0.2	
	4.0			626.4	71.4	7.8 ± 0.2	
	5.6			637.4	107.0	6.1 ± 0.2	
	6.9			65	140.8	4.7 ± 0.1	
8.5	664.0	192.0	2.9 ± 0.1				
10.3	659.8	272.8	0.8 ± 0.05				
11.2	635.5	333.4	0.2 ± 0.02				

^a The liquid and gas phase densities were calculated according to ref 13.

between the initial and the equilibrium weight change, Figure 4. Table 4 gives the densities that were used for determining the IFT from the pendant drop profiles of the crude oil in CO_2 at (313 and 353) K.

Interfacial Tension (IFT). The influences of temperature and pressure on IFT are best studied using pure binary systems. Since phase behavior is well-known in alkane mixtures and in combination with nitrogen and carbon dioxide, these systems are appropriate to show the principle differences between completely nonpolar fluids (alkanes, nitrogen) and fluids that contain a dipole or quadrupole moment like CO_2 . In Table 3 and Figure 5 the IFT of *n*-heptane is depicted in different compressed gas atmospheres. Analogous to data at 288 K from Dechoz and Roze,¹⁵ the steepest slope is observed in case of CO_2 with the IFT vanishing at the point of complete miscibility. Compared to this behavior, the IFT remains at considerably

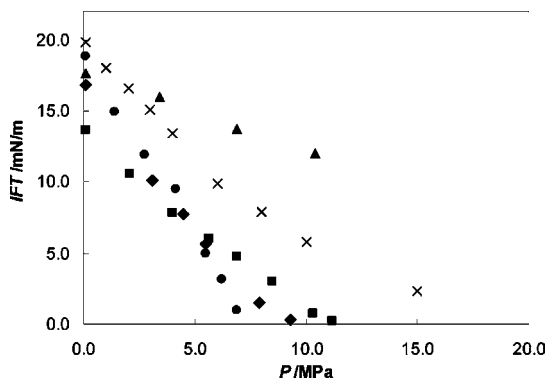


Figure 5. Effect of pressure on IFT of binary systems. ●, *n*-heptane–CO₂, 313.2 K; ◆, *n*-heptane–CO₂, 323.2 K; ■, *n*-heptane–CO₂, 353.2 K; ▲, *n*-heptane–N₂, 323.2 K; ×, *n*-heptane–CH₄, 298.2 K.

Table 4. Densities and IFT of the Crude Oil–CO₂ System^a

<i>T</i>	<i>P</i>	ρ_{liquid}	ρ_{CO_2}	IFT
K	MPa	kg·m ⁻³	kg·m ⁻³	mN·m ⁻¹
313.2	0.1	828.8 ± 0.2	1.7	25.8 ± 0.3
	2.2	837.1 ± 0.5	37.1	21.0 ± 0.3
	4.0	848.4 ± 1.0	83.8	16.0 ± 0.3
	6.1	864.9 ± 1.5	149.5	10.6 ± 0.3
	8.5	869.6 ± 2.5	279.5	4.2 ± 0.2
	1	872.1 ± 5.0	627.7	1.6 ± 0.5
353.2	0.1	799.6 ± 0.2	1.5	21.9 ± 0.3
	3.0	803.7 ± 0.8	49.3	17.1 ± 0.2
	6.0	810.2 ± 1.2	110.2	12.3 ± 0.2
	9.25	817.6 ± 2.2	195.8	7.3 ± 0.2
	12.0	822.7 ± 5.0	297.3	3.3 ± 0.5

^a The density of CO₂ was calculated according to ref 13.

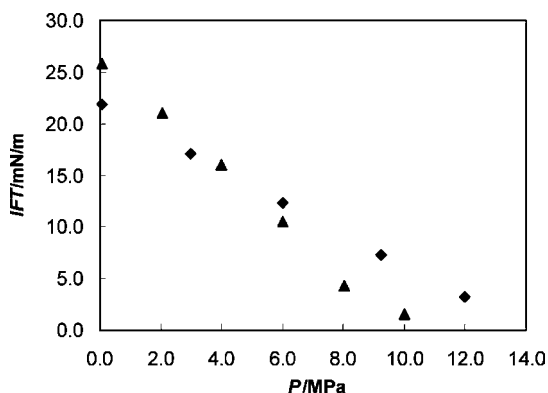


Figure 6. Effect of pressure on IFT of crude oil–CO₂; ▲ 313.2 K, ◆ 353.2 K.

higher values in case of nitrogen. The binary alkane mixture takes values in between the systems showing strong (CO₂) and little (N₂) miscibility.

Table 4 and Figure 6 show the IFT of the crude oil in CO₂ as a function of pressure. Similar to the pure binary systems, the IFT strongly decreases as the pressure rises. At low pressures the typical temperature influence is observed. At 5 MPa there is a crossover between the isotherm at 313 K and that at 353 K. At high pressures the increased miscibility at lower temperatures starts to dominate, resulting in lower IFT at lower temperatures. Yang and Gu¹⁶ find similar values of the IFT in the crude oil–CO₂ system. Surprisingly, their starting value of the IFT at 0.1 MPa does not depend on temperature, and hence, no crossover point is found.

Reservoir systems usually comprise also aqueous phases that are in contact with liquid hydrocarbons and a further fluid phase,

Table 5. Densities and IFT of the Water–Crude Oil–CO₂ System^a

	<i>T</i>	<i>P</i>	ρ_{oil}	$\rho_{\text{aqueous phase}}$	ρ_{CO_2}	IFT
aqueous phase	K	MPa	kg·m ⁻³	kg·m ⁻³	kg·m ⁻³	mN·m ⁻¹
deionized water	323.2	0.1	821.4 ± 0.5	988.2	1.6	19.5 ± 0.4
		2.76	832.4 ± 0.6	989.5	51.0	17.3 ± 0.4
		5.86	844.8 ± 0.8	990.9	130.8	14.5 ± 0.3
	353.2	9.30	858.6 ± 3.5	992.4	311.9	13.1 ± 0.3
		0.1	799.6 ± 0.2	971.9	1.5	18.6 ± 0.5
		5.51	821.3 ± 0.8	974.3	99.3	14.3 ± 0.4
seawater	323.2	0.1	821.4 ± 0.5	1026.8	1.6	19.3 ± 0.4
		4.07	837.7 ± 1.1	1028.7	80.6	16.9 ± 0.4
		5.90	844.8 ± 1.5	1029.6	130.8	15.3 ± 0.4
	353.2	9.30	858.6 ± 2.1	1031.2	311.9	14.4 ± 0.3
		11.02	865.5 ± 3.9	1032.0	507.7	14.1 ± 0.3

^a The densities of CO₂ and water were calculated according to ref 13.

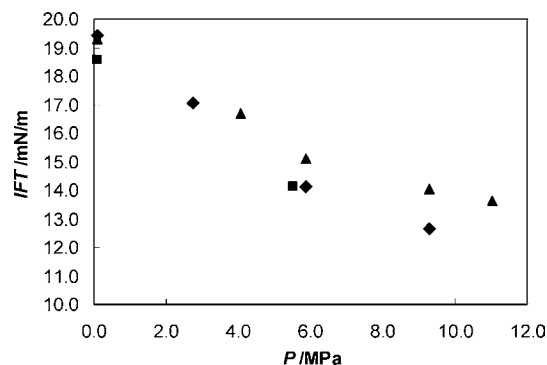


Figure 7. Effect of pressure on IFT of water–crude oil in presence of CO₂; ◆, deionized water–crude oil, 313.2 K; ■, deionized water–crude oil, 353.2 K; ▲, seawater–crude oil, 313.2 K.

which is either hydrocarbon or carbon dioxide. Table 5 and Figure 7 show data on liquid–liquid IFT in the presence of CO₂.

Hauser and Michaelis¹⁷ have shown that there is only a small effect of pressure on the IFT in immiscible liquid–liquid systems. In some cases the IFT even increases with rising pressure. Compared to this behavior, dissolved CO₂ has a clear effect on the oil–water interface resulting in decreasing values. Compared to deionized water, seawater shows slightly higher values of IFT at elevated pressures. An increasing effect of the salt on the surface tension of a liquid is already known.¹⁸ It is likely that the same effect causes slightly higher values in water–oil systems.

Contact Angle (CA). The influence of reservoir pressure on the wetting characteristics of liquid–liquid systems is of great interest, especially in the presence of CO₂. One question arising during the investigation of reservoir rock wetting is the relevance of model systems. In view of the difficulty of obtaining original rock surfaces for this type of investigation, model rocks are prepared and contacted with reservoir fluids for a defined period of time prior to the investigation. Nevertheless, it is not possible to obtain rock surfaces with exactly the same history as those of oil and gas reservoirs. Consequently, it is reasonable to focus on relative effects of varying reservoir conditions than on absolute values of contact angles.

Yang et al.⁹ presented contact angle data of a crude oil–brine–limestone system. Surprisingly, the CA presented here rises from low values representing an oil-wet situation (CA = 60°) at atmospheric conditions to water-wet CAs of around 110° at pressures above 10 MPa without CO₂ as well as in presence of CO₂. Taking into account the decreasing IFT of oil–water in the presence of compressed CO₂, a tendency toward an increasing CA is supported by Young's theory¹⁹ although absolute values cannot be given. The strong effect of

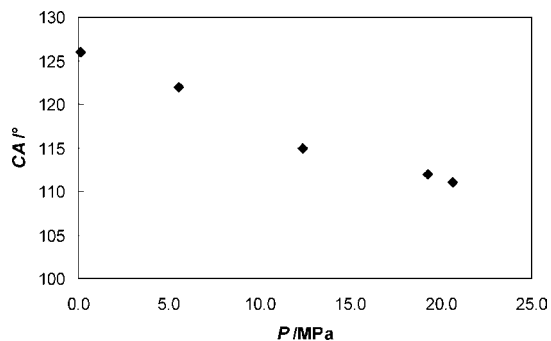


Figure 8. Effect of pressure on the CA of crude oil drop in seawater on a calcite crystal surface in the presence of CO₂, 323.2 K.

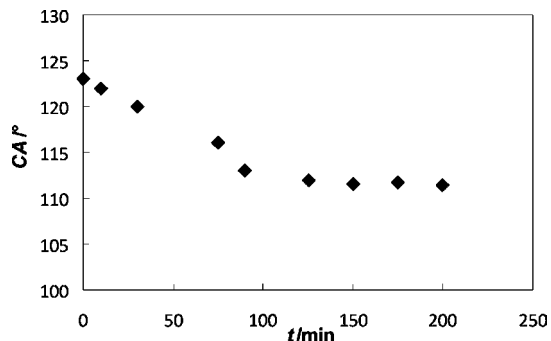


Figure 9. Evolution of the CA of crude oil in seawater on aged calcium carbonate as a function of drop age in presence of CO₂, 19.3 MPa, 323.2 K.

the pressure on the CA in the absence of CO₂ shown by the same authors is not easily comprehensible since the IFT as a key quantity between two incompressible and immiscible liquids is merely affected.

To gain more insight into this complex matter, the effect of compressed carbon dioxide on wetting was investigated. The smooth calcium carbonate crystal was chosen to start with to eliminate the effect of surface roughness and porosity, which is inherent using limestone. The aging procedure is described in the Methods section. Drops of crude oil were placed underneath the rock through a hole drilled into the rock and using a capillary sticking through this hole (Figure 2). Figure 8 shows how the CA of a drop of crude oil on a calcite crystal surface in seawater is diminished in the presence of CO₂ at rising pressure. Although quantitative information on the solid surface energies is not directly accessible, some qualitative comments can be made. According to Young's equation,¹⁹ the CA results from the relation of interfacial energies acting at the three-phase contact line. CO₂ has a considerable effect on the oil–water IFT (Figure 7), which in case of being the only effect would cause the CA to increase rather than to decrease. Hence, CO₂ dissolved within the oil drop must cause the interfacial energy between the solid and the oil to diminish. The kinetics of dissolution is related to the evolution of the CA as shown in Figure 9. After nearly 90 min of decreasing CA, a fairly constant value is established. For comparison, the CA of a drop of seawater in crude oil was also determined. Because of experimental difficulties of observing the drop profile within the almost opaque crude oil phase, the experimental error was fairly high ($\pm 3^\circ$). The resulting CA was determined as approximately 80° . Like in similar cases, the sum of both CAs is higher than 180° , which is probably due the high uncertainty and effects on a microscopic scale (surface roughness). The results show that calcium carbonate tends to be water-wet in contact with oil even though it had undergone a hydrocarbon aging procedure, while

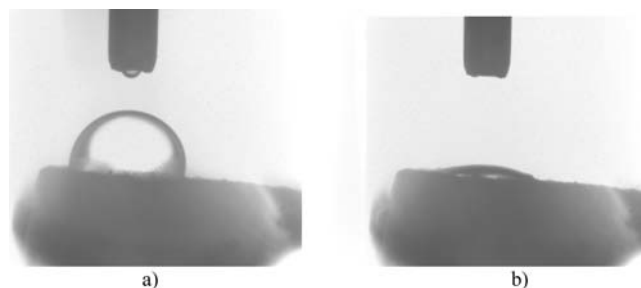


Figure 10. A drop of synthetic seawater through crude oil + CO₂ on limestone, 6.2 MPa, 323.2 K: (a) $t = 10$ min, (b) $t = 80$ min.

Table 6. CA of Crude Oil in Seawater–CO₂ on Different Rock Surfaces, 323.2 K

P [MPa]	material	CA/deg
19.3	calcium carbonate crystal	111.6 ± 1.2
19.3	limestone	109.5 ± 1.1
20.7	sandstone	134.0 ± 2.1
21.2	dolomite	100.8 ± 0.8

in an air environment oil spontaneously spreads on the contrary to water which takes a definite CA of nearly 60° .²⁰ In the real oil reservoirs, the rock is porous compared to a single even calcite crystal. Figure 10 shows a drop of seawater penetrating into a limestone in a crude oil–CO₂ atmosphere, also revealing the tendency toward water-wet. In this case no equilibrium value of the CA could be obtained.

In Table 6 CAs of oil drops observed through seawater on different surfaces are compared among each other. The CAs observed on a calcium carbonate crystal and on limestone are practically identical. Thus, in case the drop phase does not wet the surface, the porosity does not play a significant role when measuring the CA. A similar situation is produced in case of sandstone. While it is difficult to determine the CA of a water drop because it penetrates into the porous rock structure, an oil drop maintains its shape without changing. In case of dolomite an intermediate wetting situation is observed tending toward water-wet as has been shown by Jaeger and Pietsch.²¹

Conclusions

Because of its strong ability to dissolve in hydrocarbon fluids, carbon dioxide has a considerable effect on phase behavior and IFT in oil and gas reservoirs. In the presence of light hydrocarbons, complete miscibility is achieved at moderate pressures. As a consequence, the IFT decreases rapidly by increasing the pressure and ultimately vanishing at the point of complete miscibility.

IFT of crude oil in a CO₂ atmosphere significantly decreases but reveals the difference in miscibility at (313 and 353) K by exhibiting higher IFT at higher temperatures. Further, carbon dioxide has a significant effect on the IFT in a crude oil–aqueous solution system, which influences the wetting via the Young's relationship.

Dynamic studies reveal that the wetting liquid penetrates into porous rock structures, whereas drops of the nonwetting liquid maintain their shape after the adjacent liquid phases are saturated with carbon dioxide and an equilibrium CA is established.

Literature Cited

- (1) Danesch, A. Water–Hydrocarbon Interfacial Tension. In *PVT and Phase Behavior of Reservoir Fluids*; Elsevier Science B.V.: New York, 1998; Section 8.3, pp 292–294.
- (2) Yang, D.; Gu, Y. Interfacial interactions between crude oil and CO₂ under reservoir conditions. *Pet. Sci. Technol.* **2005**, *23* (9–10), 1099–1112.

- (3) Bahramian, A.; Danesh, A.; Gozalpour, F.; Tohidi, B.; Todd, A. C. Vapor-liquid interfacial tension of water and hydrocarbon mixture at high pressure and high temperature conditions. *Fluid Phase Equilib.* **2007**, *252*, 66–73.
- (4) Hansen, G.; Hamouda, A. A.; Denoyel, R. The effect of pressure on contact angles and wettability in the mica/water/*n*-decane system and the calcite + stearic acid/water/*n*-decane system. *Colloids Surf., A* **2000**, *172*, 7–16.
- (5) Lubetkin, S. D.; Akhtar, M. The variation of surface tension and contact angle under applied pressure of dissolved gases and the effect of these changes on bubble nucleation. *J. Colloid Interface Sci.* **1996**, *180*, 43–60.
- (6) Jaeger, P.; Eggers, R.; Baumgartl, H. Interfacial properties of high viscous liquids in a supercritical carbon dioxide atmosphere. *J. Supercrit. Fluids* **2002**, *24*, 203–217.
- (7) Jaeger, P.; Eggers, R. Liquid-liquid interphases at high pressures in presence of compressible fluids. *Thermochim. Acta* **2005**, *438*, 16–21.
- (8) Rao, D. N. Measurements of dynamic contact angles in solid-liquid-liquid systems at elevated pressures and temperatures. *Colloids Surf., A* **2002**, *206* (1–3), 203–216.
- (9) Yang, D.; Gu, Y.; Tontiwachwuthikul, P. Wettability determination of the crude oil–reservoir brine–reservoir rock system with dissolution of CO₂ at high pressures and elevated temperatures. *Energy Fuels* **2008**, *22* (4), 2362–2371.
- (10) Wu, Y.; Shuler, P. J.; Blanco, M.; Tang, Y.; Goddard, W. A. An Experimental Study of Wetting Behavior and Surfactant EOR in Carbonates with Model Compounds. *SPE J.* **2008**, 99612.
- (11) Nasr-El-Din, H. A.; Al-Othman, A.; Taylor, K. C.; Al-Ghamdi, A. Surface Tension of Acid Stimulating Fluids at High Temperatures. *J. Petrol. Sci. Eng.* **2004**, *1–2* (43), 57–73.
- (12) Song, B.; Springer, J. Determination of Interfacial Tension from the Profile of a Pendant Drop Using Computer-Aided Image Processing. *J. Colloid Interface Sci.* **1996**, *184*, 64–76.
- (13) Kunz, O.; Klimeck, R.; Wagner, W.; Jaeschke, M. The GERG-2004 Wide-Range Equation of State for Natural Gases and Other Mixtures. *VDI Fortschrittber.* **2004**, *6*, 557.
- (14) Yang, G. C. C.; Drzymala, J. Aqua-oleophilicity and Aqua-oleophobicity of Solid Surfaces. *Colloids Surf.* **1986**, *17*, 313–315.
- (15) Dechoz, J.; Roze, C. Surface tension measurement of fuels and alkanes at high pressure under different atmospheres. *Appl. Surf. Sci.* **2004**, *229*, 175–182.
- (16) Yang, D.; Gu, Y. Visualization of Interfacial Interactions of Crude Oil–CO₂ Systems under Reservoir Conditions. *SPE J.* **2004**, 89366.
- (17) Hauser, E. A.; Michaelis, A. S. Interfacial Tension at Elevated Pressure and Temperature. A New and Improved Method Apparatus for Boundary Tension Measurements by the Pendant Drop Method. *J. Phys. Colloid Chem.* **1948**, *52*, 1157–1165.
- (18) Aggelopoulos, C. A.; Robin, M.; Perfetti, E.; Vizika, O. CO₂/CaCl₂ solution interfacial tensions under CO₂ geological storage conditions: Influence of cation valence on interfacial tension. *Adv. Water Resour.* **2010**, *33* (6), 691–697.
- (19) Young, T. An Essay on the Cohesion of Fluids. *Philos. Trans. R. Soc. London* **1805**, *95*, 65–87.
- (20) Wang, W.; Gupta, A. Investigation of the effect of temperature and pressure on wettability using modified pendant drop method. *SPE J.* **1995**, 30544.
- (21) Jaeger, P.; Pietsch, A. Characterization of reservoir systems at elevated pressure. *J. Petrol. Sci. Eng.* **2009**, *64*, 20–24.

Received for review August 9, 2010. Accepted October 10, 2010. The authors would like to thank Saudia Arabia Oil Company for funding this project.

JE100825B